Critical role of CXCL4 in the lung pathogenesis of influenza (H1N1) respiratory infection

L Guo[1,3], K Feng[1,3], YC Wang[1,3], JJ Mei[1,2], RT Ning[1], HW Zheng[1], JJ Wang[1], GS Worthen[2], X Wang[1], J Song[1], QH Li[1] and LD Liu[1]

Annual epidemics and unexpected pandemics of influenza are threats to human health. Lung immune and inflammatory responses, such as those induced by respiratory infection influenza virus, determine the outcome of pulmonary pathogenesis. Platelet-derived chemokine (C-X-C motif) ligand 4 (CXCL4) has an immunoregulatory role in inflammatory diseases. Here we show that CXCL4 is associated with pulmonary influenza infection and has a critical role in protecting mice from fatal H1N1 virus respiratory infection. CXCL4 knockout resulted in diminished viral clearance from the lung and decreased lung inflammation during early infection but more severe lung pathology relative to wild-type mice during late infection. Additionally, CXCL4 deficiency decreased leukocyte accumulation in the infected lung with markedly decreased neutrophil infiltration into the lung during early infection and extensive leukocyte, especially lymphocyte accumulation at the late infection stage. Loss of CXCL4 did not affect the activation of adaptive immune T and B lymphocytes during the late stage of lung infection. Further study revealed that CXCL4 deficiency inhibited neutrophil recruitment to the infected mouse lung. Thus the above results identify CXCL4 as a vital immunoregulatory chemokine essential for protecting mice against influenza A virus infection, especially as it affects the development of lung injury and neutrophil mobilization to the inflamed lung.

INTRODUCTION

Influenza A virus (IAV) infections cause respiratory diseases in large populations worldwide every year and result in seasonal influenza epidemics and unexpected pandemic. IAV enters hosts through upper respiratory infections. After first proliferating in the respiratory epithelium, the virus destroys the epithelial cells and induces the extravasation of protein-rich tissue fluid into the alveoli and trachea, which, in severe cases, causes viral pneumonia and lung edema, impairing the gas exchange function of the lungs.[1] When IAV infects the respiratory system, the innate immune system responds first; the infected epithelial and immune cells release inflammatory cytokines to recruit large numbers of granulocytes, macrophages, and monocytes to the lung parenchyma and alveoli. These innate immune cells clear the virus via phagocytosis and the dissolution of infected cells while releasing cytokines and inflammatory chemokines, such as interferon (IFN)-γ, tumor necrosis factor (TNF)-α, interleukin (IL)-6, and IL-1β, to exert further antiviral innate immune effects.[2] Meanwhile, the innate immune cells act as antigen-presenting cells and release cytokines to activate the adaptive cellular and humoral immune responses, further clearing the virus.[3] However, severe lung inflammation and tissue damage caused by an excessive infection-induced immune response are often the main cause of death in the clinic. The killing effect of excess macrophages and neutrophils, as well as the resulting cytokine storm, gives rise to acute lung injury and acute respiratory distress syndrome.[4,5] Determining how to control viral infection and proliferation while preventing injury caused by the immune system itself remains a challenge in respiratory infections.

Chemokine (C-X-C motif) ligand 4 (CXCL4), also known as platelet factor 4 (PF4), is primarily stored in platelet α-granules and released upon activation of platelet aggregation. Research

[1]Department of Viral Immunology, Institute of Medical Biology, Chinese Academy of Medical Science and Peking Union Medical College, Kunming, China and [2]Division of Neonatology, Department of Pediatrics, Children's Hospital of Philadelphia, Perelman School of Medicine, University of Pennsylvania, Philadelphia, Pennsylvania, USA. Correspondence: LD Liu (longdingl@gmail.com)
[3]These authors contributed equally to this work.

Received 31 October 2016; accepted 31 December 2016; published online 25 January 2017. doi:10.1038/mi.2017.1

concerning the biological function of CXCL4 has revealed that this protein has a role in suppressing hematopoiesis, platelet aggregation and wound repair, inhibiting endothelial cell proliferation and angiogenesis, and regulating immune and inflammatory responses.[6,7] Although CXCL4 was the first member of the CXC chemokine family to be identified, purified CXCL4 has no chemotactic activity for neutrophils *in vitro*.[6] Basically, this protein binds to C-X-C motif chemokine receptor 3 (CXCR3) and glycosaminoglycans but not the neutrophil chemotaxis receptor CXCR2.[7] Nevertheless, other studies have found that CXCL4 can enhance neutrophil adherence to endothelial cells and facilitate neutrophil exocytosis to release myeloperoxidase and lysozyme.[7] With regard to immunoregulation, CXCL4 also shows a cellular immune effect in facilitating neutrophil recruitment to inflamed tissues,[8–12] promoting the activation, proliferation, and differentiation of monocytes,[13,14] natural killer cells,[15] dendritic cells,[16] and T cells.[17,18]

The role of CXCL4 in immunoregulation has been investigated in inflammatory bowel disease,[19] hepatic fibrosis,[12] bacterial pneumonia,[8] and mesenteric ischemia/reperfusion injury.[10] Owing to its dual regulatory roles in immune response and inflammation, this protein may have a physiological function in respiratory viral infectious diseases, such as IAV infection. In this work, we constructed a CXCL4 knockout ($CXCL4^{-/-}$) mouse model of respiratory IAV infection and investigated the biological role of CXCL4 in the course of IAV infection.

RESULTS

CXCL4 is required for the survival of mice infected with fatal doses of H1N1 influenza virus

Ten-to-12 week-old male $CXCL4^{-/-}$ mice and wild-type (WT) C57BL/6 mice were infected intranasally with the H1N1 PR8 virus (2,000 50% cell culture infective dose ($CCID_{50}$) each) after anesthesia; mice instilled with phosphate-buffered saline (PBS) served as negative controls. With the indicated challenge dose, WT and $CXCL4^{-/-}$ mice began to lose body weight gradually after infection, and $CXCL4^{-/-}$ mice showed more significant weight loss than WT mice (**Figure 1a**). Meanwhile, viral infection resulted in marked differences in the survival rates of the two groups of mice. With a body weight $<80\%$ (7–9 days postinfection (d.p.i.)), approximately 42% of the WT mice died (survival rate, 58%). The body weight slowly recovered in WT mice that survived longer than 9 d.p.i., and no deaths occurred after that time (**Figure 1a,b**). $CXCL4^{-/-}$ mice also died at 7 d.p.i., and the mortality rate reached 50%. All the $CXCL4^{-/-}$ mice died at 11 d.p.i., with no survivors (**Figure 1b**). To determine the CXCL4-specific effects in the CXCL4 null mice, $CXCL4^{-/-}$ mice were given recombinant PF4 protein (5 μg per mouse) on day 0 and daily postinfection. Exogenous CXCL4 increased the survival rate of $CXCL4^{-/-}$ mice to a level slightly higher than that in WT infected mice (**Figure 1c**). Additionally, we measured CXCL4 expression in the systemic blood circulation and locally in the lungs of IAV infected mice. H1N1 infection led to CXCL4 release into the sera of WT mice upon infection (peak value at 3–5 d.p.i., approxomately 35 $\mu g\,ml^{-1}$), followed by a slow decline as the mice gradually recovered from infection (**Figure 1d**). Immunohistochemical analysis of the lungs of WT mice revealed that CXCL4 was mainly localized in the blood and around the blood capillaries (**Figure 1e**). In contrast, H1N1 infection led to increased expression of CXCL4 in the lungs of WT mice, as a large proportion of this protein was distributed in the lung interstitium and alveolar walls (**Figure 1e**). No obvious CXCL4 expression was detected in the sera or lung tissues of $CXCL4^{-/-}$ mice throughout the course of infection (**Figure 1d,e**). Taken together, these results suggest that CXCL4 has an important role in protecting mice against fatal H1N1 respiratory infection.

H1N1 influenza virus infection of $CXCL4^{-/-}$ mice contributes to more severe lung inflammatory injury

To determine whether the high mortality of $CXCL4^{-/-}$ mice caused by H1N1 infection was due to acute lung injury or other reasons, we analyzed the pathological changes in the lung tissue, the extent of lung edema, and the protein concentrations in the lung bronchoalveolar lavage fluid (BALF) from mice during the early and late stages of infection. Hematoxylin and eosin staining of the lung tissue revealed the presence of lung inflammation in both WT and $CXCL4^{-/-}$ mice relative to their control counterparts at 3 d.p.i. The symptoms included inflammatory cell infiltration into the lung parenchyma and interstitium and massive inflammatory cell aggregation in the alveolar walls and spaces (**Figure 2a**). Unlike $CXCL4^{-/-}$ mice, WT mice also presented a noticeable thickening of the bronchial epithelium, substantial accumulation of inflammatory cells, and more significant alveolar expansion after infection (**Figure 2a**). During late infection (9 d.p.i.), the lung inflammation gradually resolved in the surviving WT mice, with the alveolar structure tending to be complete and only a small number of inflammatory cells aggregating around the bronchial epithelium (**Figure 2a**). However, disruption of the alveolar structure and the formation of a hyaline membrane were observed in the lungs of dying $CXCL4^{-/-}$ mice during late infection (**Figure 2a**). The results of the semiquantitative analysis of lung injury and the histological score suggested that $CXCL4^{-/-}$ mice have fewer pathological changes in the lung during early infection but develop more severe lung damage during late infection than WT infected mice (**Figure 2a**). Furthermore, the lung wet-to-dry weight ratios of both groups of infected mice were markedly increased at 3 d.p.i., and WT mice had slightly higher values than $CXCL4^{-/-}$ mice (**Figure 2b**). At 9 d.p.i., the lung wet-to-dry ratios had decreased in the WT mice but remained relatively high in $CXCL4^{-/-}$ mice and were higher than the levels observed at 3 d.p.i. (**Figure 2b**). This result shows that the $CXCL4^{-/-}$ mice developed more severe lung edema following infection. Moreover, analysis of protein concentrations and inflammatory cytokine levels in the lung BALF was performed. The results showed that, at 3 d.p.i., the protein concentrations in the lung BALF were significantly higher in

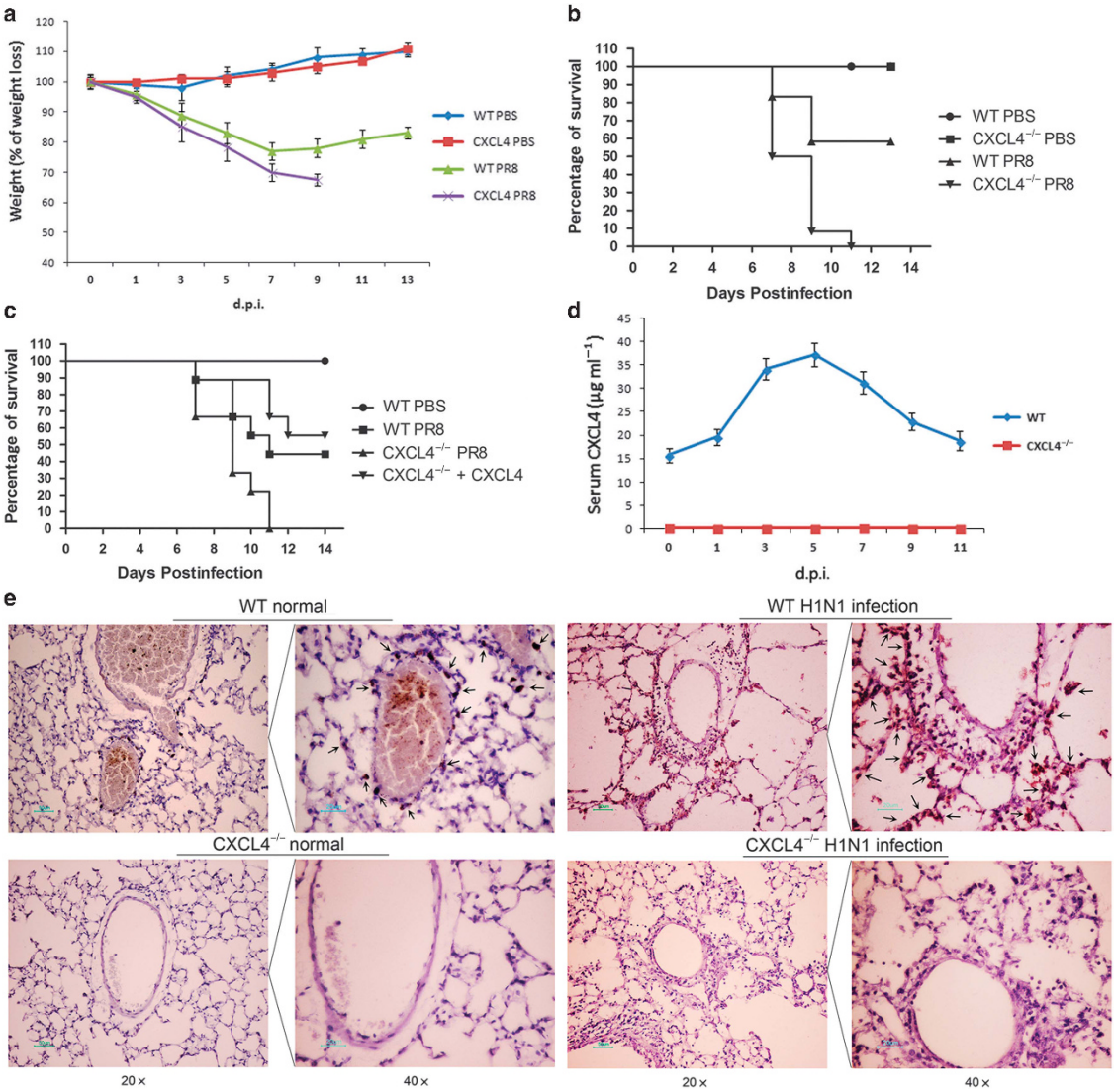

Figure 1 Chemokine (C-X-C motif) ligand 4 (CXCL4) is essential for mouse survival after infection with a fatal dose of H1N1 influenza virus. Wild-type (WT) and CXCL4$^{-/-}$ mice were infected intranasally with a fatal dose of the H1N1 A/PR/8 virus (2,000 $CCID_{50}$) (50% cell culture infective dose); phosphate-buffered saline (PBS) instillation was used as a control. (**a**) Body weight loss ($n = 12$) of the mice was monitored until 2 week postinfection. (**b**) Kaplan–Meier survival curve for the infected mice ($n = 12$) is shown. (**c**) Kaplan–Meier survival curve for the infected mice receiving intravenous injection of recombinant CXCL4 protein ($n = 9$). (**d**) CXCL4 levels in the sera of infected mice ($n = 4$) were determined. (**e**) Lung sections from normal and infected WT and CXCL4$^{-/-}$ mice were stained at 3 days postinfection (d.p.i.) with an anti-CXCL4 antibody and hematoxylin. The arrows in each graph point to the obvious expression of CXCL4. Error bars represent the s.d., $^*P < 0.05$ based on Student's *t*-test.

both groups of infected mice (nearly 1,000 μg ml^{-1}) than in their control counterparts (**Figure 2c**). At 9 d.p.i., the protein concentrations in the CXCL4$^{-/-}$ mice further increased to >2,000 μg ml^{-1}, which was significantly higher than that in WT infected mice (**Figure 2c**). Enzyme-linked immunosorbent assay (ELISA) showed that CXCL4$^{-/-}$ mice had significantly lower TNF-α, IL-1β, and IL-6 levels than WT mice at 3 d.p.i. but higher levels of IL-6 and TNF-α at 9 d.p.i. (**Figure 2d**). These data suggest that CXCL4 deficiency altered the release of inflammatory cytokines in the infected mouse lungs. Collectively, the above results indicate that, although lung inflammation and pathology were decreased in the lungs of CXCL4 deficiency, H1N1-infected mice during early infection, lung pathology was continuously exacerbated during the progression of infection and caused severe lung edema and lung injury at the late stage of infection.

CXCL4 deficiency impairs viral clearance from the lungs of H1N1-infected mice

Next we quantified viral replication and proliferation in the lung tissue of infected mice using viral titer and load tests. The results showed that the variations in viral titers and viral loads following infection were consistent with each other. The viral titers and loads reached high levels in both WT and CXCL4$^{-/-}$ mice at 3 d.p.i. (approximately 10^6 $CCID_{50}$ ml^{-1} and 10^6 copies per 100 ng RNA, respectively) (**Figure 3a,b**).

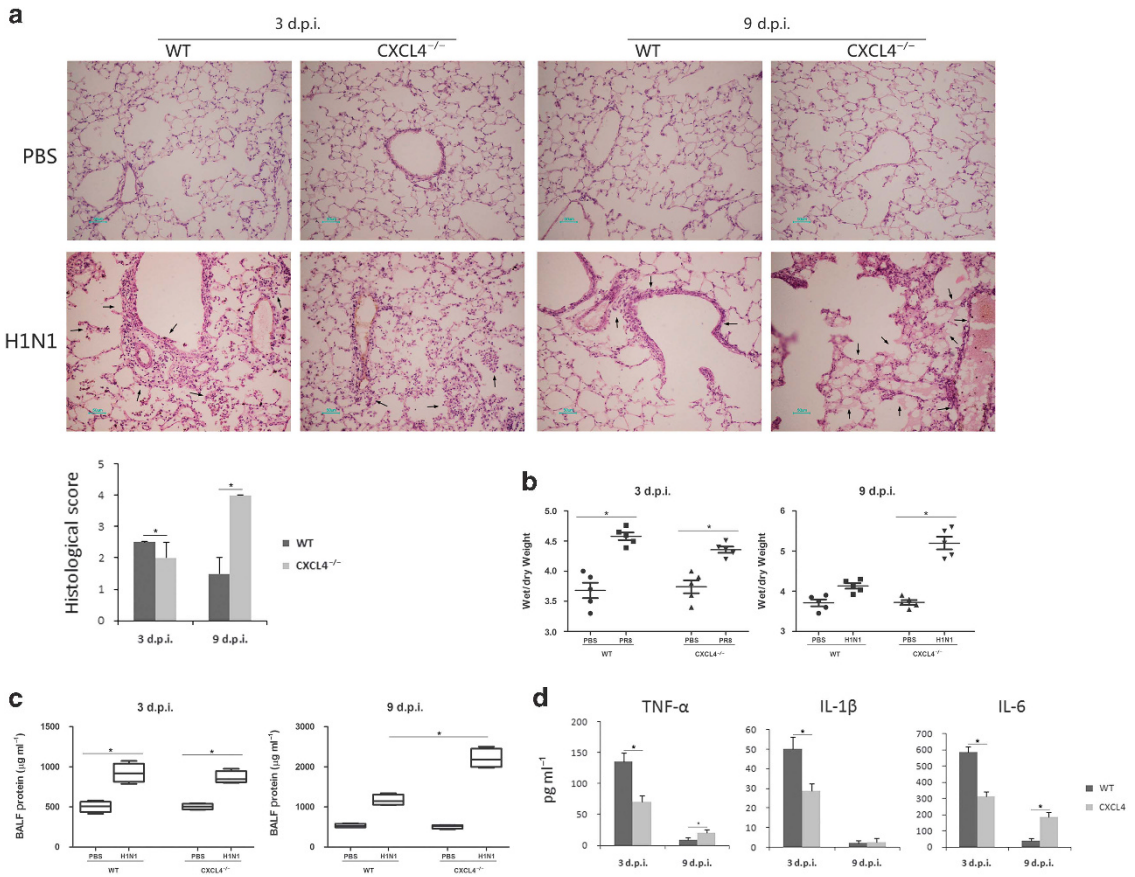

Figure 2 Severe lung damage in CXCL4$^{-/-}$ mice after H1N1 influenza virus infection. Wild-type (WT) and CXCL4$^{-/-}$ mice were infected intranasally with the H1N1 A/PR/8 virus (2,000 $CCID_{50}$) (50% cell culture infective dose), and phosphate-buffered saline (PBS) was instilled as a control. (**a**) Histopathology of hematoxylin and eosin–stained lung sections from WT and CXCL4$^{-/-}$ mice 3 and 9 days postinfection (d.p.i.). Arrows indicate thickening of the bronchial epithelium and inflammatory cell aggregation (WT, 3 d.p.i.), inflammatory cell infiltration and accumulation (CXCL4$^{-/-}$, 3 d.p.i.), inflammatory cell aggregation around the bronchial epithelium (WT, 9 d.p.i.), and hyaline membrane formation (CXCL4$^{-/-}$, 9 d.p.i.). Lung histological scores were assessed by a blinded veterinary pathologist as described in the Methods section. (**b**) Infected mouse lung wet-to-dry ratios were used to assess lung edema at 3 and 9 d.p.i. (**c**) The total protein concentrations in the bronchoalveolar lavage fluid (BALF) of infected mouse lungs were determined at 3 and 9 d.p.i. (**d**) Levels of the inflammatory cytokines tumor necrosis factor (TNF)-α, interleukin (IL)-1β, and IL-6 were measured using an enzyme-linked immunosorbent assay. Error bars represent the s.d. of five samples. *$P<0.05$ based on Student's *t*-test. CXCL4, chemokine (C-X-C motif) ligand 4.

Both the viral titers and loads of WT mice began to decline at 5 d.p.i., and the virus was cleared to <10 $CCID_{50}$ ml^{-1} in WT mice at 11 d.p.i. However, in CXCL4$^{-/-}$ mice, viral proliferation continued at 5 d.p.i., and the viral titers remained at high levels of no $<10^5$ at 7 d.p.i. The viral titers and loads of CXCL4$^{-/-}$ mice began to fall at 7 d.p.i., but the virus remained at a titer of no $<10^4$ and a load of no $<10^5$ at 9 d.p.i. (**Figure 3a,b**). This result reveals that, in comparison to WT mice, CXCL4$^{-/-}$ mice failed to effectively clear the H1N1 influenza virus following infection, resulting in delayed viral clearance with a large amount of virus in the lungs 1 week postinfection.

CXCL4$^{-/-}$ mice exhibit an altered innate immune response with insufficient neutrophil infiltration into the lung alveoli after H1N1 infection

The clearance of IAV respiratory infection depends on the activation of a series of innate and adaptive immune cells. To address the antiviral immune response, we continuously monitored the composition of immune cells in the lung BALF of WT and CXCL4$^{-/-}$ infected mice. First, the results showed that the number of leukocytes in the BALF from infected WT mice increased sharply during the initial stages of infection and peaked at 5 d.p.i. (10^8–10^9 ml^{-1}) before decreasing gradually (**Figure 4a**). In CXCL4$^{-/-}$ mice, the number of leukocytes also increased drastically but was significantly lower than that in WT mice at 3 and 5 d.p.i. (approximately 10^6–10^7 ml^{-1}). The number of leukocytes in the BALF of CXCL4$^{-/-}$ mice dropped at 7 d.p.i. but rose to a peak value at 9 d.p.i. (10^7–10^8 ml^{-1}) (**Figure 4a**). Next we conducted cell smearing and counting for different immune cells in the lung BALF. During early infection (3 and 5 d.p.i.), both the percentage and number of neutrophils in the lung BALF were significantly lower in CXCL4$^{-/-}$ mice than in WT mice; in contrast, the percentages and numbers of macrophages and lymphocytes were higher in CXCL4$^{-/-}$ mice than in WT mice (**Figure**

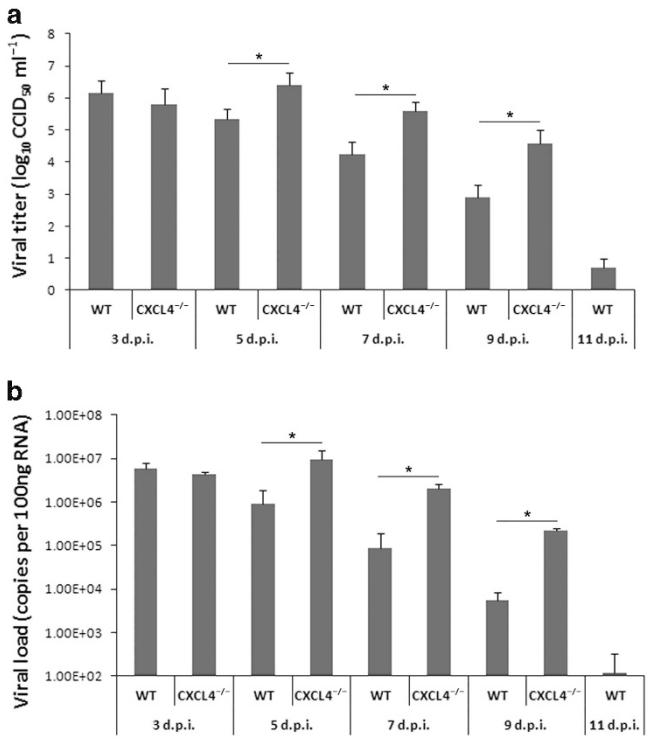

Figure 3 Chemokine (C-X-C motif) ligand 4 (CXCL4) knockout results in impaired viral clearance. Lungs were harvested from H1N1 A/PR/8 (2,000 $CCID_{50}$) (50% cell culture infective dose) infected wild-type (WT) and $CXCL4^{-/-}$ mice, and homogenates were prepared for viral titers and loads. (**a**) Titers of infectious virus were determined using a standard $CCID_{50}$ assay at different days postinfection (d.p.i.). (**b**) Viral loads were determined based on the number of influenza M gene RNA copies detected by real-time reverse transcriptase–PCR at different d.p.i. Error bars represent the s.d. of triplicate samples. $^*P < 0.05$ based on Student's *t*-test.

4b–d and **Supplementary Figure S1** online). During late infection (7–11 d.p.i.), the percentages of neutrophils and macrophages decreased gradually following infection, while the number of lymphocytes showed an upward trend in both groups (**Supplementary Figure S1**). At 9 d.p.i., the number of leukocytes in $CXCL4^{-/-}$ mice increased, leading to a significantly greater number of three types of immune cells in $CXCL4^{-/-}$ mice relative to WT mice, especially the lymphocytes (**Figure 4a–d Supplementary Figure S1**). In short, $CXCL4^{-/-}$ mice had fewer BALF leukocytes than WT mice during early infection, primarily owing to significantly reduced neutrophil infiltration into the lungs. During late infection, the number of leukocytes was still high in the lung BALF of $CXCL4^{-/-}$ mice, mainly owing to the presence of abundant lymphocytes.

The adaptive immune response has a critical role in viral clearance during late infection. Thus we further detected the lung virus-specific cellular immune response and humoral immune response at the late stage of infection (9 d.p.i.). We isolated lymphocytes from the lung-draining mediastinal lymph node and quantified the numbers of CD4+, CD8+, and CD19+ lymphocytes by flow cytometry. No significant differences in the numbers of T and B lymphocytes were found between $CXCL4^{-/-}$ and WT mice (**Figure 4e**). We challenged the isolated lymphocytes with the H1N1 virus, and subsequent flow cytometric analysis revealed no significant differences in the percentages of CD8+ and IFN-γ+ cells in the two groups of mice (**Figure 4f**). Keeping with these results, the staining of BALF cells with CD3+, CD4+, CD8+, and IFN-γ antibodies showed that the average frequencies of CD4+, CD8+, and CD8+/IFN-γ cells were similar in WT and $CXCL4^{-/-}$ mice and that, owing to the large number of lymphocytes accumulated in the BALF, $CXCL4^{-/-}$ mice showed a greater number of CD4+, CD8+, and CD8+/IFN-γ cells than WT mice (see **Supplementary Figure S2**). Moreover, the lung BALF T helper type 1 (Th1) and Th2 cytokine levels in the infected mice were analyzed using the Bio-Plex Mouse Cytokine Th1/Th2 Assay. The levels of both the Th1 effector cytokine IFN-γ and the Th2 effector cytokines IL-4, IL-5, and IL-10 tended to be consistent in WT and $CXCL4^{-/-}$ mice (**Figure 4g**). Additionally, an influenza hemagglutination inhibition assay revealed no significant differences in specific antibodies against H1N1 in the sera from the two groups of infected mice (**Figure 4h**). In summary, CXCL4 deficiency decreased the antiviral innate immune response in the mouse lung during early H1N1 infection, with a significantly reduced number of neutrophils; CXCL4 knockout did not affect the activation of the viral-specific adaptive immune response, but did contribute to the accumulation of lymphocytes in the lung BALF during late infection.

CXCL4 facilitates neutrophil recruitment to the lungs of H1N1-infected mice

Neutrophils have important roles in controlling fatal influenza infection in our H1N1 PR8 mouse model of respiratory infection, as depletion of neutrophils with a specific anti-Ly6G antibody resulted in impaired lung viral clearance, more severe lung pathology, and extremely high mortality (see **Supplementary Figure S3**). To address how CXCL4 deficiency correlates with decreased neutrophil accumulation in the lung BALF from infected mice, we further analyzed the recruitment of neutrophils into the lungs of mice infected with influenza. Myeloperoxidase activity, which is a specific marker of activated neutrophils, was measured in lung tissue homogenates and appeared to be significantly lower in $CXCL4^{-/-}$ mice than in WT mice at 3 and 5 d.p.i. (**Figure 5a**). The murine chemokines keratinocyte-derived chemokine (KC; CXCL1) and macrophage inflammatory protein-2 (MIP-2; CXCL2) are the major chemoattractants responsible for recruiting neutrophils; we found that both KC and MIP-2 levels in the lung BALF were lower in $CXCL4^{-/-}$ mice, with the MIP-2 level being significantly lower than that in WT mice at 3 and 5 d.p.i. (**Figure 5b**). To further determine the direct effects of CXCL4 on neutrophil recruitment to the lung, an atraumatic orotracheal intubation method was used to intratracheally administer purified CXCL4 protein.[20] The results showed that the instillation of CXCL4 increased the number of alveolar neutrophils in both WT mice (approximately 15-fold) and $CXCL4^{-/-}$ mice (approximately 10-fold) (**Figure 5c**). CXCR2

has been described as the main neutrophil chemokine receptor in mice. When we treated mice with a CXCR2 antagonist before the administration of CXCL4, the CXCL4-triggered recruitment of neutrophils into the lung BALF of both WT and CXCL4$^{-/-}$ mice was reduced to a level close to that in the negative control mice receiving PBS instillation (**Figure 5c**).

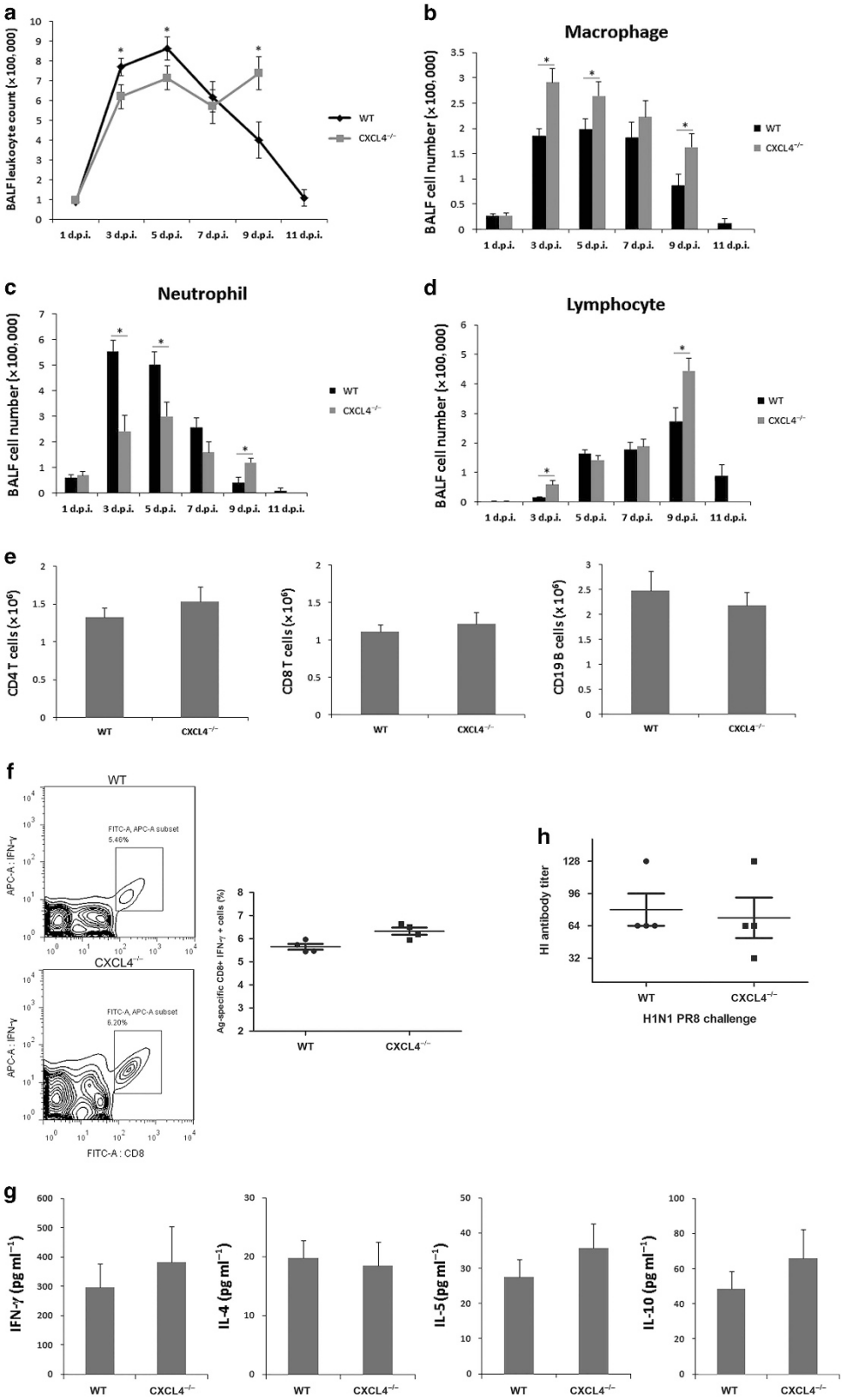

These results indicated that CXCL4 regulates neutrophil infiltration into the mouse lung. Meanwhile, both KC and MIP-2 levels in the lung BALF after CXCL4 administration were significantly increased than control groups in both WT and CXCL4$^{-/-}$ mice (**Figure 5c**). Neutrophils are generated in the bone marrow, and mature neutrophils are released into the blood and migrate into peripheral organs and tissues. We used flow cytometry to detect the Gr-1 + cell population in the bone marrow of infected mice and found no differences in the percentage or number of cells in this population between WT and CXCL4$^{-/-}$ mice at 3 and 5 d.p.i. (see **Supplementary Figure S4**). Additionally, the cytokine granulocyte colony-stimulating factor (G-CSF) has been shown to have an important role in the generation and maturation of bone marrow neutrophils. When comparing the levels of G-CSF in the peripheral blood of the two groups of mice, we found that CXCL4$^{-/-}$ mice had slightly but not significantly higher levels of G-CSF than WT mice at 3 and 5 d.p.i. (see **Supplementary Figure S4**). These results suggest that CXCL4 deficiency did not affect the generation of neutrophils in the bone marrow of the infected mice. When comparing the numbers of neutrophils in the peripheral blood of the two groups of mice, we found that CXCL4$^{-/-}$ mice had fewer neutrophils than WT mice; however, the difference between the groups did not reach significance (**Figure 5d**). After H1N1 infection, the number of neutrophils was significantly lower in CXCL4$^{-/-}$ mice than in WT mice at 3 and 5 d.p.i. (**Figure 5d**). The above results implied that CXCL4 deficiency could be a pivot of neutrophil recruitment from the bone marrow to the circulation and inflamed lung. By testing the serum levels of KC and MIP-2 from the infected mice, we found that both chemokines were significantly lower in CXCL4$^{-/-}$ mice than in WT mice at 3 and 5 d.p.i. (**Figure 5e**). Similarly, after intravenous injection of exogenous PF4 in CXCL4$^{-/-}$ mice, both serum levels of KC and MIP-2 were significantly increased compared with non-injected CXCL4$^{-/-}$ mice at 3 d.p.i. (**Figure 5f**). In addition, by comparing the expression of the CXCR2 receptor on blood neutrophils, we found that CXCR2 expression in CXCL4$^{-/-}$ mice is similar to that in WT mice (**Figure 5g**). After H1N1 infection, the circulating neutrophils of CXCL4$^{-/-}$ mice exhibited greater CXCR2 expression than WT mice (**Figure 5g**). These data suggest that CXCL4 deficiency decreased the release of neutrophil chemokines upon influenza infection and lower concentrations of CXCR2 ligands in the serum of CXCL4$^{-/-}$ mice than that of WT mice, given greater upregulation of surface CXCR2 expression on blood neutrophils of the former. Altogether, the above results indicate that CXCL4 contributes to neutrophil recruitment to the lungs of H1N1-infected mice.

CXCL4 is dispensable for neutrophils from H1N1-induced death

To determine whether the decreased neutrophil accumulation in the infected lung BALF of CXCL4$^{-/-}$ mice is also owing to the neutrophil death in the infected lung, we used flow cytometry to detect cell apoptosis and necrosis in the infected lung BALF. The results showed no difference between WT and CXCL4$^{-/-}$ mice in the total number of leukocyte survival (**Figure 6a,b**). When comparing the number of neutrophil survival via Gr-1 gating, CXCL4$^{-/-}$ mice showed lower numbers than WT mice but without statistical significance (**Figure 6a,b**). To further determine that neutrophil survival is correlated to CXCL4 itself, neutrophils were isolated from uninfected WT mice and incubated *in vitro* with or without CXCL4 protein under normal conditions or H1N1 PR8 infection. The results showed that CXCL4 had no effect on neutrophil survival and apoptosis in normal culture or under H1N1 infection (**Figure 6c,d**). Thus these results suggest that CXCL4 does not affect neutrophil survival alone or under H1N1 infection.

DISCUSSION

Using a CXCL4 knockout mouse model of fatal influenza H1N1 respiratory infection, we first showed that CXCL4 is correlated with respirovirus infection. Pulmonary infection by the influenza virus induces CXCL4 expression systemically and locally in the infected lung. Loss of CXCL4 resulted in high mortality of H1N1-infected mice, and the restoration of CXCL4 *in vivo* rescued the phenotype of infected CXCL4$^{-/-}$ mice, suggesting that CXCL4 has a critical role in protecting against respiratory infection by influenza virus. CXCL4 deficiency exacerbates lung inflammation and pathology following infection and causes severe lung injury and edema at the end. Experimental evidence have shown that CXCL4 contributes to tissue damage in inflammatory diseases, such as acute pancreatitis,[11] abdominal sepsis,[9] mesenteric ischemia/reperfusion injury,[10] liver fibrosis,[12] and lipopolysaccharide-induced acute lung injury.[8] In these models, the reduction in tissue damage caused by loss of CXCL4 function seems to result from reduced inflammatory cell infiltration and inflammatory cytokine release, which suggests that

Figure 4 Chemokine (C-X-C motif) ligand 4 (CXCL4) knockout alters the accumulation of bronchoalveolar lavage fluid (BALF) immunocytes without affecting activation of lung adaptive immunity after H1N1 influenza virus infection. Wild-type (WT) and CXCL4$^{-/-}$ mice were infected with H1N1 influenza virus (2,000 $CCID_{50}$) (50% cell culture infective dose) on day 0, and the BALF and lymphocytes from the lung-draining mediastinal lymph node of the infected mice were collected and analyzed at the indicated time points postinfection. (**a**) The total number of leukocytes in the BALF was counted. (**b**–**d**) The total number of macrophages (**b**), neutrophils (**c**) and lymphocytes (**d**) was determined. (**e**) The total number of CD4 + T cells, CD8 + T cells, and CD19 + B cells in the mediastinal lymph nodes at 9 days postinfection (d.p.i.) were determined by flow cytometry. (**f**) The percentage of CD8 + and interferon (IFN)-γ + cells in the mediastinal lymph node lymphocytes collected at 9 d.p.i. was determined by flow cytomtery. (**g**) The levels of the T helper type 1 (Th1) and Th2 effector cytokines IFN-γ, interleukin (IL)-4, IL-5, and IL-10 were measured using the Bio-Plex Mouse Cytokine Th1/Th2 Assay. (**h**) The sera of infected mice were collected at 9 d.p.i., and the hemagglutination inhibition titers of the sera against H1N1 A/PR/8 were evaluated. Error bars represent the s.d. of four samples. $^*P<0.05$ based on Student's *t*-test.

inflammation is attenuated in the inflamed tissues. Indeed, our results found reduced lung inflammation with fewer lung pathological changes and decreased inflammatory cell infiltration into the lung and inflammatory cytokine accumulation in CXCL4$^{-/-}$ mice compared with WT mice during early H1N1 infection. However, the lung inflammation and pathology

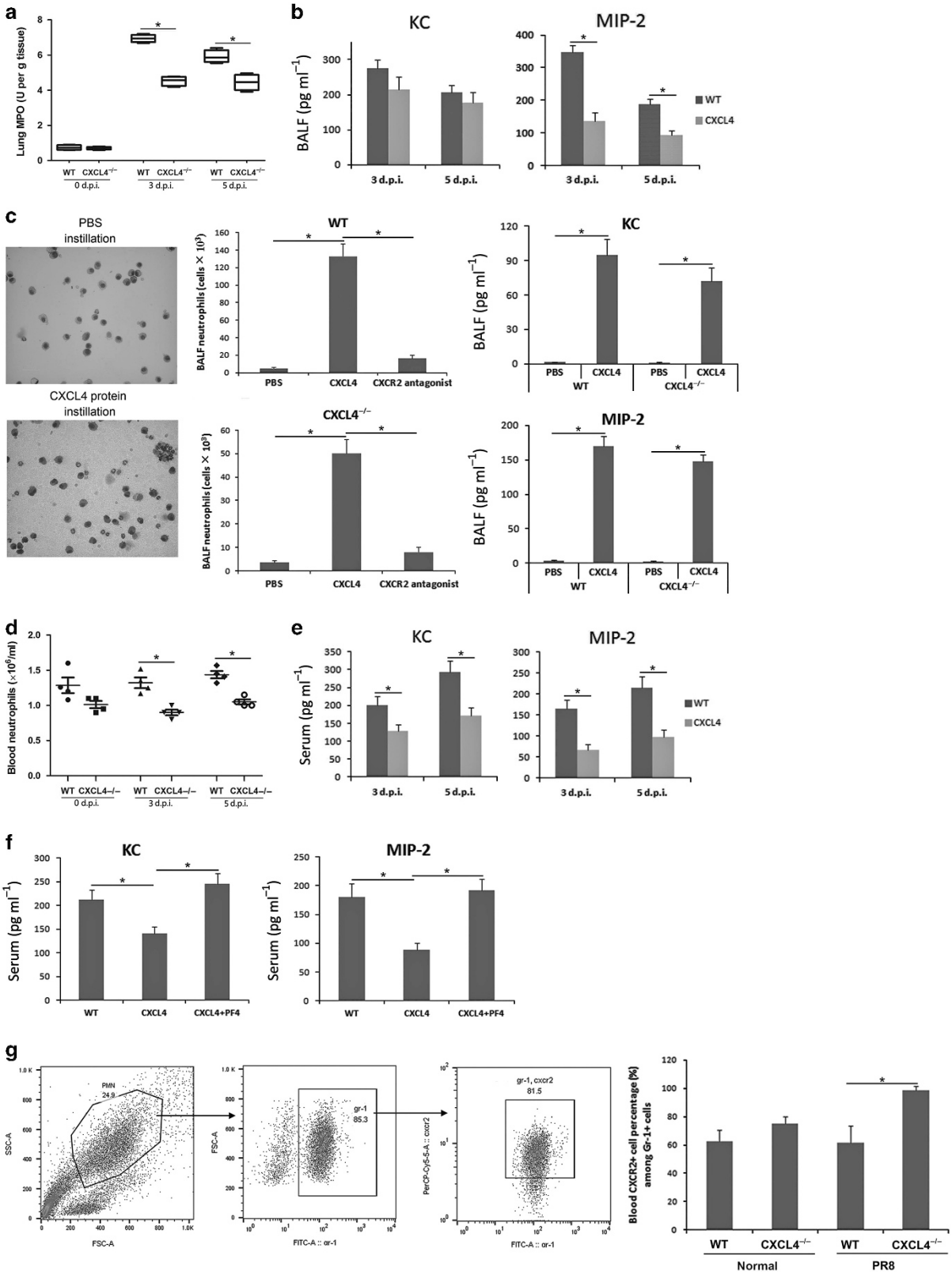

were not resolved in CXCL4$^{-/-}$ mice as they were in WT mice following infection; rather, they continued to worsen. This was probably due to the impaired viral clearance in CXCL4$^{-/-}$ mice, as both viral proliferation and infection were still higher in these mice than in WT mice after infection; this may stimulate an excessive immune-mediated inflammatory response in the infected lung and result in severe inflammatory lung injury.

CXCL4$^{-/-}$ mice failed to effectively clear the virus from the infected lung, suggesting that CXCL4 affects the pulmonary antiviral immune response in the body. Analysis of the immune cells in the infected mouse lungs showed a significant difference in the cells in CXCL4$^{-/-}$ and WT mice. Specifically, during early infection (3 and 5 d.p.i.), CXCL4$^{-/-}$ mice exhibited a significantly lower percentage and number of neutrophils in the BALF but increased numbers of macrophages relative to WT mice. The increase in macrophages did not compensate for the significant decrease in neutrophils, resulting in an overall lower level of leukocytes in CXCL4$^{-/-}$ mice. During late infection, the number of macrophages and neutrophils decreased, and lymphocytes became the predominant cell type in the BALF, mediating the adaptive antiviral immune response in the infected mouse lung. CXCL4 deficiency did not affect the activation of pulmonary viral-specific T and B lymphocytes in the infected mice, as the number of H1N1-specific CD8+ cells in the mediastinal lymph node and BALF, BALF levels of IFN-γ, BALF Th1/Th2 response, and serum viral-specific antibody levels were not lower than those in infected WT mice. Because of the large number of lymphocytes that accumulated in the BALF of CXCL4$^{-/-}$ mice, the number of CD4+, CD8+, and H1N1-specific CD8+ cells was statistically greater than that in infected WT mice during late infection (9 d.p.i.) (see **Supplementary Figure S2**). These results suggest that CXCL4 deficiency did not affect the activation of viral-induced T and B lymphocytes in the influenza-infected lung. CXCL4 has been reported to stimulate and activate T cells in cultured lymphocytes,[17,18] and it is possible that viral infection has a major role in stimulating and activating T cells in the infected lung. Meanwhile, it seems that the impaired viral clearance is not due to the pulmonary antiviral adaptive immune response. Indeed, the viral loads and titers continuously decreased during late infection (5–9 d.p.i.) (**Figure 3**). The delayed viral clearance seems to be correlated with the antiviral innate immune response, especially the reduced neutrophil accumulation in the lungs of infected CXCL4$^{-/-}$ mice. Although neutrophils were initially speculated to contribute to lung injury and mortality, abundant evidence has shown that neutrophils have a protective role during IAV infection; neutrophils exert direct and indirect antiviral effects by absorbing the virus, killing the virus via extracellular traps, and facilitating the adaptive immune response.[21–25] In our respiratory H1N1 PR8-infected mouse model, we confirmed the protective effect of neutrophils via antibody-mediated depletion. The results also showed diminished lung viral clearance during infection and abundant inflammatory cell infiltration into the lung alveolar spaces during late infection, which is similar to our infected CXCL4$^{-/-}$ mouse model (see **Supplementary Figure S3**). The predominant inflammatory cells in the lung BALF were mainly lymphocytes and macrophages, suggesting that neutrophil depletion contributes to increased lymphocyte and macrophage accumulation in the influenza-infected mouse lung. Thus, as for the neutrophil-mediated facilitation of the adaptive immune response, it is possible that the presence of large amounts of virus in the lungs of CXCL4$^{-/-}$ mice directly activated the immune response of T and B lymphocytes. Additionally, the persistent presence of numerous macrophages and monocytes may promote the activation of T and B lymphocytes in the lungs of CXCL4$^{-/-}$ mice during the infection process.

The decreased neutrophil infiltration into the infected lungs of CXCL4-deficient mice indicates that CXCL4 affects neutrophil recruitment to the inflamed lung tissue. Indeed, studies on inflammatory diseases have suggested that CXCL4 facilitates neutrophil recruitment to the inflamed tissues.[8,9] We further analyzed neutrophil homeostasis in CXCL4 knockout mice upon respiratory influenza infection. The data showed that CXCL4 deficiency does not affect neutrophil generation in the bone marrow after viral infection (see **Supplementary Figure S4**). The loss of CXCL4 decreases the number of circulating neutrophils in the blood of infected mice, suggesting that CXCL4 contributes to neutrophil release from bone marrow upon lung inflammation. By testing neutrophil apoptosis and death in the infected lung BALF, the results showed that survival of neutrophil is slightly lower in CXCL4$^{-/-}$ than in WT mice. However, further *in vitro* survival assays showed that

Figure 5 Chemokine (C-X-C motif) ligand 4 (CXCL4) contributes to neutrophil recruitment to the H1N1-infected mouse lung. Wild-type (WT) and CXCL4$^{-/-}$ mice were killed before H1N1 influenza virus challenge or at 3 or 5 days postinfection (d.p.i.). (**a**) The lungs were harvested, and homogenates were prepared for the myeloperoxidase (MPO) test. (**b**) The levels of keratinocyte-derived chemokine (KC) and macrophage inflammatory protein-2 (MIP-2) in the infected lung bronchoalveolar lavage fluid (BALF) were measured using an enzyme-linked immunosorbent assay (ELISA). (**c**) The numbers of neutrophils and the levels of KC and MIP-2 in the lung BALF of WT and CXCL4$^{-/-}$ mice after atraumatic orotracheal instillation with CXCL4 was assessed with or without C-X-C motif chemokine receptor 2 (CXCR2) antagonist administration before CXCL4 challenge as described in the Methods section. (**d**) Blood was collected into EDTA-coated tubes via retro-orbital bleeding, and the neutrophil numbers were determined using a Hemavet 950 Automated Veterinary Analyzer. (**e**) The levels of KC and MIP-2 in the serum were measured using an ELISA assay. (**f**) The levels of KC and MIP-2 in the serum of infected mice with intravenous injection of CXCL4 as described in the Methods section were measured using an ELISA assay. (**g**) Blood was stained with anti-Gr-1-FITC (fluorescein isothiocyanate) and anti-CXCR2-PerCP antibodies after lysis of red cells. The Gr-1+ CXCR2+ cell population was gated as illustrated, and the number of cells was dertermined by flow cytometry. Error bars represent the s.d. of four samples. *$P<0.05$ based on Student's *t*-test. FSC, forward scatter; PBS, phosphate-buffered saline; SSC, side scatter.

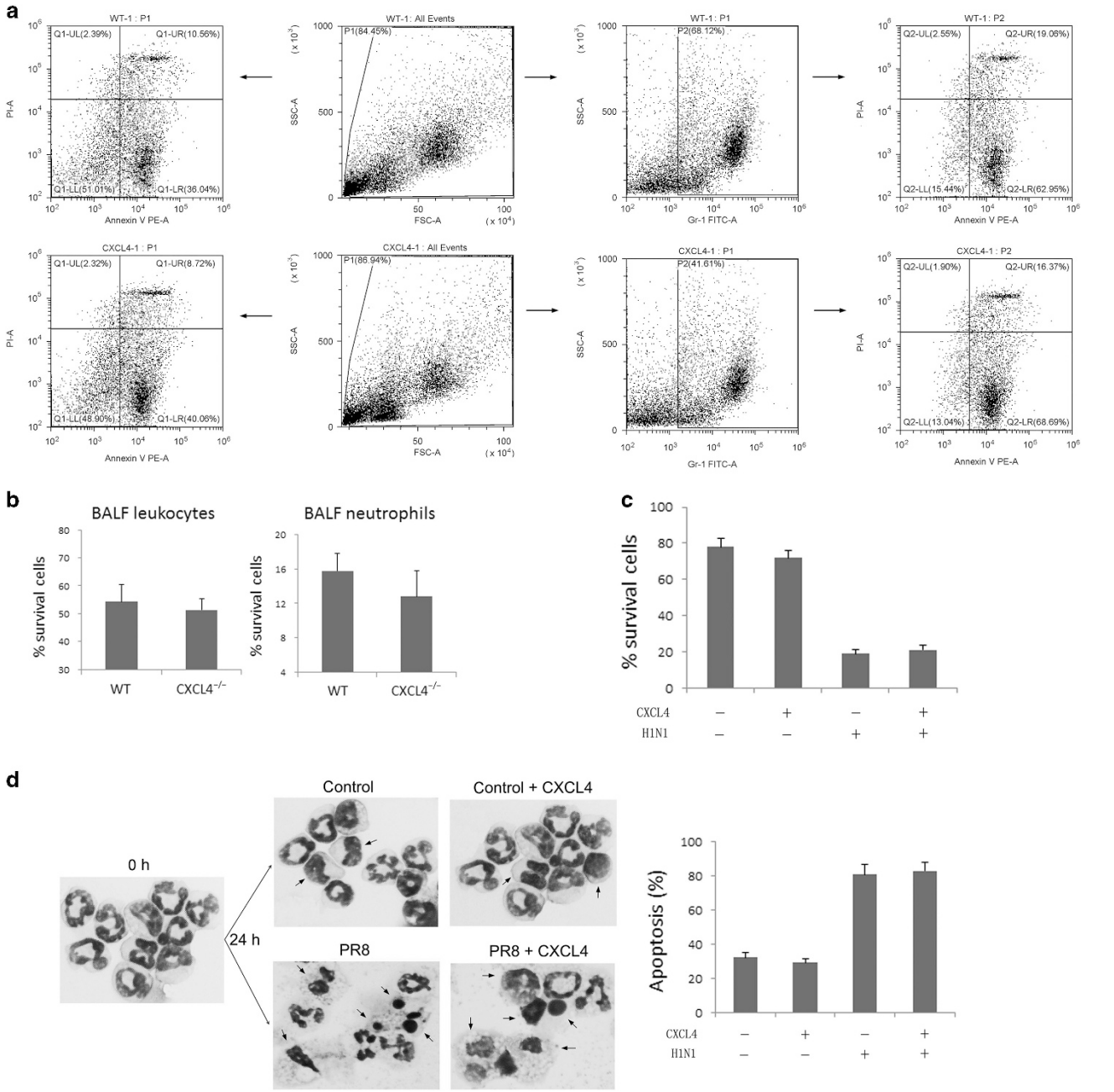

Figure 6 Effects of chemokine (C-X-C motif) ligand 4 (CXCL4) on neutrophil survival and apoptosis. (**a**) Bronchoalveolar lavage fluid (BALF) cells were collected from H1N1 A/PR/8 (2,000 $CCID_{50}$) (50% cell culture infective dose) infected wild-type (WT) and $CXCL4^{-/-}$ mice at 3 days postinfection (d.p.i.), and analyzed by flow cytometry using Gr-1-FITC (fluorescein isothiocyanate), Annexin V-PE (phycoerythrin), and PI (propidium iodide) staining. (**b**) The percentage of survival cells in the infected lung BALF were counted from the Q1-LL or Q2-LL subpopulations. Neutrophils were aseptically collected from the peripheral blood of C57BL/6 mice and cultured *in vitro* in the absence (control) or presence of CXCL4 protein with or without H1N1 infection for 24 h. (**c**) The survival rates of cultured neutrophils were determined by trypan blue staining. (**d**) Apoptosis of cultured neurophils was determined by morphological assessment as described in the Methods section. Arrows point to apoptosis neutrophils with denser nuclei and vacuolation. Error bars represent the s.d. of triplicate samples. $^{*}P<0.05$ based on Student's *t*-test.

CXCL4 has no effects on neutrophil survival or apoptopsis in normal culture conditions or under H1N1 infection. These results indicate CXCL4 alone is dispensable for neutrophil survival. Certainly, these results do not rule out the possibility that neutrophil survival in the infected mouse lung is affected by CXCL4 deficiency. Loss of CXCL4 altered the expression of inflammatory cytokines in the infected lung BALF, as the expression of IL-6, which is important for the survival of neutrophils in the influenza-infected mouse lung, decreased at 3 d.p.i.[26] Thus CXCL4 deficiency may affect the survival of infiltrating neutrophils via secondary effect on inflammatory release in the influenza-infected mouse lung rather than having a direct effect itself.

The levels of neutrophil chemokines KC and MIP-2 were compared between WT and CXCL4$^{-/-}$ mice during H1N1 infection. The serum levels of KC and MIP-2 were significantly lower than those in WT mice. In line with this, the neutrophil chemokine receptor CXCR2 was upregulated on the surface of circulating neutrophils in infected CXCL4$^{-/-}$ mice, which suggests a lower level of CXCR2 ligands in the blood relative to infected WT mice. Similarily, the BALF levels of KC and MIP-2 were lower in CXCL4$^{-/-}$ mice than WT mice. By giving ectogenous CXCL4 into the infected CXCL4$^{-/-}$ mice, the results suggested increased KC and MIP-2 levels in the blood. Also, direct administering of CXCL4 into the normal CXCL4$^{-/-}$ mouse lung induces the expression of KC and MIP-2 in the BALF. These results demonstrated that CXCL4 spurs mouse KC/MIP-2–CXCR2 neutrophil chemotaxis pathway. CXCR2 is the only functional receptor mediating neutrophil influx into inflamed tissues in mice, and CXCL1 and CXCL2 have been suggested to be the two most important chemokines for neutrophil recruitment into the inflamed and respirovirus-infected lung in rodents.[27–30] Interesting, CXCL4 does not bind to CXCR2 but to CXCR3, and CXCL4 itself has no chemotactic activity for neutrophils *in vitro*.[6,7] CXCR3 is a Gα_i protein-coupled receptor that consists of two variants CXCR3-A and CXCR3-B, and only CXCR3-B binds to CXCL4.[7] CXCR3 is expressed primarily on activated lymphocytes, macrophages, dendritic cells, natural killers, inflamed neutrophils, and some epithelial and endothelial cells. Rare expression on rest T, B lymphoctes and neutrophils.[31–34] It is possible that CXCL4 binds to CXCR3 expressed on the cells mentioned above and induces the expression of KC and MIP-2 in these cells. In turn, the expression of KC and MIP-2 will fulfill neutrophil recruitment through CXCR2 pathway. Indeed, CXCR3 pathway has been found to contribute to the development of neutrophil-mediated fulminant lung injury of viral and nonviral origin, and CXCR3$^{-/-}$ mice showed decreased neutrophil infiltration in the H1N1-infected mouse lung BALF.[33] Besides, Hwaiz *et al.*[9] have revealed recently that CXCL4 promote macrophage secretion of CXCL2. Future work is needed to elucidate CXCL4–CXCR3 axis induces CXCL1/CXCL2–CXCR2 pathway.

Overall, our results suggest a critical role of CXCL4 in respiratory influenza infection. The role of CXCL4 in viral infection–induced lung pathology is not similar to its role in inflammatory diseases, in which CXCL4 ameliorates tissue inflammation and damage; rather, CXCL4 deficiency aggravates lung inflammation and injury in the infected lung and contributes to mortality of the infected mice. This difference is probably due to the altered immune-inflammatory response in the influenza-infected mouse lung, which is mediated primarily by neutrophil recruitment to the inflamed lung.

METHODS

Animals and virus. CXCL4$^{-/-}$ mice[35] and WT control C57BL/6 mice were obtained from Dr G. Scott Worthen at Children's Hospital of Philadelphia. The mice were bred and housed in individually ventilated cages at the Central Animal Care Services of the Institute of Medical Biology, Chinese Academy of Medical Sciences, under specific-pathogen-free conditions. Male mice aged 10–12 weeks were used in all the experiments. The mouse-adapted A/Puerto Rico/8/1934 H1N1 (A/PR/8) influenza virus was stored in our laboratory. The virus was grown in the chorioallantoic fluid of 9-day-old embryonated chicken eggs. The viral titer was determined from the $CCID_{50}$ in Madin–Darby canine kidney (MDCK) cells using the method of Reed and Muench.

Mouse infection model. WT and CXCL4 knockout mice were anesthetized by intraperitoneal injection of pentobarbital (50 mg per body weight) and then inoculated intranasally with 2,000 $CCID_{50}$ of influenza virus in 30 µl PBS (PBS alone as a control). Weight loss was monitored, and survival curves were generated. To demonstrate CXCL4-specific effects in the CXCL4$^{-/-}$ mice, H1N1-infected CXCL4$^{-/-}$ mice were given recombinant CXCL4 (5 µg per mouse) (OriGene, Beijing, China) on day 0 and daily postinfection by intravenous injection via the retro-orbital plexus as described previously,[36] the survival of the CXCL4-restored mice was determined, and the serum levels of KC and MIP-2 were determined by ELISA. All the animal experiments were conducted under prior approval from the animal ethics committee of the Institute of Medical Biology, Chinese Academy of Medical Sciences, with permit number [2014] 43, according to the national guidelines on animal work in China.

Orotracheal challenge with CXCL4. An atraumatic orotracheal intubation method was used to intrtracheally administer purified CXCL4 protein.[20] Briefly, WT or CXCL4$^{-/-}$ mice were anesthetized and orotracheally intubated with a 20-gauge angiocatheter with the guidance of an optical fiber source. Mice were subsequently placed in a vertical position suspended by their upper incisors. A polyethylene catheter was advanced into the trachea and used to instill either purified CXCL4 protein (1 µg in 30 µl sterile PBS) or sterile PBS as a control. Four hours after CXCL4 administration, the BALF was collected as described below for analysis of the number of neutrophils and the levels of KC and MIP-2. In the CXCR2 antagonist experiments, a CXCR2 antagonist (SB225002, 4 µg g^{-1}) (Selleck Chemicals, Houston, TX) or vehicle (PBS) was administered intraperitoneally 10 min prior to the orotracheal administration of CXCL4.

Viral loads and titers. Mice were killed every 2 days following intranasal infection, and lung tissue samples were harvested, and the weights of tissues were recorded. Samples were mechanically homogenized using a TGrinder instrument (TIANGEN Biotechnologies, Beijing, China), and RNA was isolated using TRNzol A + reagent (TIANGEN Biotechnologies). The RNA concentration of each sample was determined by UV 260/280 using NanoDrop 2000 (ThermoFisher Scientific, Waltham, MA). In all, 100 ng of total RNA was reverse transcribed and amplified using the One Step PrimeScript RT-PCR Kit (TAKARA Biotechnologies, Dalian, China) on an Applied Biosystems 7500 Real-Time PCR System (Life Technologies, Waltham, MA). To determine the viral loads, primers and a probe for the viral matrix protein gene (M gene) were used: 5′-AAGACCAA TCCTGTCACCTCTGA-3′ (forward), 5′-CAAAGCGTCTACGCTG CAGTCC-3′ (reverse), and 5'-(FAM)-TTTGTGTTCACGCTCACC GT-(TAMRA)-3' (probe). The M genes of the A/PR/8 viruses were cloned into the pMD18-T vector, which was used to create a standard curve by 10-fold serial dilution. Viral copy numbers were normalized to the mass of the original tissue samples and calculated based on the standard curve described above. The RNA samples from each individual were quantified in triplicate.

Lung homogenates were centrifuged at 5,000 r.p.m. for 10 min at 4 °C, and the supernatants were collected. Viral titers were determined using $CCID_{50}$ titers by serial titration of viruses in MDCK cells. Titers were calculated by the method of Reed and Muench.

BALF cells and total proteins. The mice were first anesthetized, killed, and bled thoroughly. After the trachea was exposed, the lungs were

lavaged four times with 0.8 ml of cold, sterile PBS, and the BALF was centrifuged at 1500 g for 10 min at 4 °C. Supernatants were collected and stored at − 80 °C for protein, chemokine, and cytokine detection. All of the leukocytes in the BALF were counted and resuspended at 10^5 cells ml^{-1} in PBS. In all, 200 µl of these solutions was cytospun onto slides, and the cells were stained with the Wright's–Giemsa Stain Kit (Nanjing Jiancheng Bioengineering, Jiangsu, China) for differential leukocyte count in five random fields under a microscope.

Lung histological, immunohistochemical analyses, and wet/dry weight. Mice were killed, and the lungs were slowly inflated by instilling 1 ml of 4% formaldehyde intratracheally. The trachea was tightened, and the lungs were fixed in formalin for 48 h at 4 °C and embedded in paraffin. Lung tissue sections (5 µm) were stained with hematoxylin and eosin according to routine procedures for histological analysis. The lung histological score was measured by a blinded pathologist with a 0–4 point scale according to the combined assessments of alveolar structure, inflammatory cell infiltration, and aggregation in the alveolar space and septa, bronchiolitis, and lung edema. A score of 0 represented no damage; 1 represented mild damage; 2 represented moderate damage; 3 represented severe damage; and 4 represented very severe histological changes; an increment of 0.5 was used if the levels of inflammation fell between two integers. In each tissue sample, three random areas were scored, and the mean value was calculated. The histology score is the median value from four mice. For immunohistochemical studies, sections were stained with a mouse monoclonal CXCL4/PF4 antibody (R&D Systems, Minneapolis, MN) overnight at 4 °C, and tissue sections were subsequently incubated with an horseradish peroxidase–conjugated goat anti-mouse secondary antibody (OriGene) for 30 min and counterstained with hematoxylin. Images were obtained with a light microscope (Nikon, Tokyo, Japan).

Mouse lungs were harvested and weighed immediately (wet weight). The lung tissue was then dried in an oven at 60 °C for 72 h and reweighed to determine the dry weight. The wet-to-dry weight ratio was calculated for each animal to assess tissue edema.

Hemagglutination inhibition assay. Sera were prepared from the blood of infected mice at 9 d.p.i. Before the test, any non-specific inhibitors of hemagglutination were removed by diluting sera with receptor-destroying enzyme (Denka Seiken, Tokyo, Japan) at a ratio of 1:5 and incubating the samples at 37 °C overnight. The enzyme was inactivated by a 2-h incubation at 56 °C followed by the addition of 0.1% sodium citrate. The hemagglutination inhibition assay was performed using the A/PR/8 strain with 1% chicken erythrocytes in V-bottom 96-well microtiter plates.

Flow cytometry. BALF cells were collected as described before. The blood, bone marrows, and mediastinal lymph nodes were collected at the time of necropsy. Single-cell suspensions were obtained by flushing the bone marrow or gently pressing the lymph node against a 70-µm strainer into PBS. Cells were washed in fluorescence-activated cell sorter buffer after lysis with ACK buffer. Cell surface staining was performed using anti-mouse Gr-1-FITC (fluorescein isothiocyanate), CD3-PerCP, CD4-PE (phycoerythrin), CD8-FITC, CD19-APC (allophycocyanin) (BD Biosciences, Franklin Lakes, NJ) and CXCR2-PerCP (R&D Systems). For the influenza-specific CD8+ cells, mediastinal lymph node cells or BALF cells were stimulated overnight with formalin-inactivated Influenza A PR/8/34 H1N1 (multiplicity of infection = 2). Brefeldin A (1 µM) was added after overnight stimulation, and the cells were incubated for an additional 5 h. Later, cells were surface stained with anti mouse CD3-PerCP and CD8-FITC and then permeabilized with Cytofix–Cytoperm solution (BD Biosciences) and stained with intracellular anti-mouse IFN-γ–APC. Flow cytometric data were collected on a FACS Canto (BD Biosciences) and analyzed using the FlowJo version 10.1 (Ashland, OR). For determining neutrophil apoptosis in the infected lung BALF, BALF cells were analyzed by CytoFLEX (Beckman Coulter, Indianapolis, IN) using the Gr-1-FITC, Annexin V–phycoerythrin (BD Biosciences) and propidium iodide (Solarbio, Beijing, China) staining.

MPO assay. Lung MPO activity was determined using an MPO Detection Kit (Nanjing Jiancheng Bioengineering). Briefly, tissue was homogenized in 1 ml of 50 mmol l^{-1} PBS (pH 6.0) containing 0.5% hexadecyltrimethylammonium hydroxide and centrifuged at 12,000 r.p.m. min^{-1} at 4 °C for 20 min. In all, 10 µl of the supernatant was transferred into PBS (pH 6.0) containing 0.17 mg ml^{-1} 3, 3′-dimethoxybenzidine and 0.0005% H_2O_2. The MPO activity in the supernatant was determined by measuring the H_2O_2-dependent oxidation of 3,3′-dimethoxybenzidine; the reaction was read at an optical density of 450 nm with a Synergy 4 (BioTek, Winooski, VT). Values were expressed as MPO units per gram of tissue.

Neutrophil depletion. C57BL/6 mice were intraperitoneally injected with 500 µg of rat anti-Ly6G [1A8] antibody (Abcam, Cambridge, UK) or isotype control antibody to deplete neutrophils *in vivo*. Mice were treated 24 h before infection and every 48 h thereafter. Depletion of neutrophils (>90%) from the blood was confirmed by differential leukocyte counts (data not shown). The survival rates, H1N1 viral loads, and lung pathologies of neutrophil-depleted mice were assessed.

Cytokine assays. The Bio-Plex Suspension Array System (Bio-Rad, Hercules, CA) was used to evaluate BALF cytokine levels. The Mouse Cytokine Th1/Th2 Assay was used to evaluate IL-4, IL-5, IL-10, and IFN-γ levels according to the user manual. The concentrations of cytokines, G-CSF, TNF-α, IL-1β, IL-6, KC, MIP-2, and CXCL4 in mouse BALF and sera were determined with ELISA kits (Neobioscience, Beijing, China) in accordance with the manufacturer's instructions.

In vitro neutrophil survival assays. Neutrophils were aseptically isolated from the the peripheral blood of normal C57BL/6 mice through a combination of dextran sedimentation and centrifugation through discontinuous plasma-Percoll gradients. Neutrophils were resuspended at 1.5×10^6 cells ml^{-1} in RPMI 1640 medium supplemented with 5% fetal calf serum and 2 mmol l^{-1} L-glutamine at 37 °C in the absence (control) or presence of purified CXCL4 protein (50 ng ml^{-1}) (OriGene) with or without H1N1 PR8 virus (multiplicity of infection = 8). After 24 h, live cells were counted by trypan blue staining. Cytospun neutrophils were stained with Wright's–Giemsa stain, and the cells were assessed for morphological changes characteristic of apoptosis (nuclear condensation, vacuolation), with the use of a ×40 objective. At least 300 cells per slide were counted.

Statistical analyses. We performed all the statistical analyses with the GraphPad Prism software (version 4, La Jolla, CA). The data that were obtained from all experiments are presented as the mean ± s.d., and $P < 0.05$ was considered to be statistically significant using Student's *t*-test.

SUPPLEMENTARY MATERIAL is linked to the online version of the paper at http://www.nature.com/mi

ACKNOWLEDGMENTS

We thank Mrs Yuhong Liu and Ning Dai for technical assistance in mouse necropsy and flow cytometry. This work was supported by the National Natural Science Foundation of China (31300143, 81373142, 31570900), the Yunnan Applied Basic Research Projects (2013FZ128 and 2015FB139), and CAMS Innovation Fund for Medical Sciences (2016-I2M-1-014). The funders had no role in study design, data collection and analysis, decision to publish, or preparation of the manuscript.

AUTHOR CONTRIBUTIONS

L.G. and L.L. conceived and designed the experiments. L.G., K.F., Y.W., R.N., J.S., and X.W. performed the experiments. J.M., Q.L., and L.L. analyzed the data. Y.W., J.M., J.W., G.W., and H.Z. contributed reagents/materials/analysis tools. L.G. and L.L. wrote the paper.

DISCLOSURE

The authors declared no conflict of interest.

REFERENCES

1. La Gruta, N.L., Kedzierska, K., Stambas, J. & Doherty, P.C. A question of self-preservation: immunopathology in influenza virus infection. *Immunol. Cell Biol.* **85**, 85–92 (2007).
2. Iwasaki, A. & Pillai, P.S. Innate immunity to influenza virus infection. *Nat. Rev. Immunol.* **14**, 315–328 (2014).
3. Braciale, T.J., Sun, J. & Kim, T.S. Regulating the adaptive immune response to respiratory virus infection. *Nat. Rev. Immunol.* **12**, 295–305 (2012).
4. Ramsey, C. & Kumar, A. H1N1: viral pneumonia as a cause of acute respiratory distress syndrome. *Curr. Opin. Crit. Care* **17**, 64–71 (2011).
5. Short, K.R., Kroeze, E.J., Fouchier, R.A. & Kuiken, T. Pathogenesis of influenza-induced acute respiratory distress syndrome. *Lancet Infect. Dis.* **14**, 57–69 (2014).
6. Kasper, B. & Petersen, F. Molecular pathways of platelet factor 4/CXCL4 signaling. *Eur. J. Cell Biol.* **90**, 521–526 (2011).
7. Vandercappellen, J., Van Damme, J. & Struyf, S. The role of the CXC chemokines platelet factor-4 (CXCL4/PF-4) and its variant (CXCL4L1/PF-4var) in inflammation, angiogenesis and cancer. *Cytokine Growth Factor Rev.* **22**, 1–18 (2011).
8. Grommes, J. *et al.* Disruption of platelet-derived chemokine heteromers prevents neutrophil extravasation in acute lung injury. *Am. J. Respir. Crit. Care Med.* **185**, 628–636 (2012).
9. Hwaiz, R., Rahman, M., Zhang, E. & Thorlacius, H. Platelet secretion of CXCL4 is Rac1-dependent and regulates neutrophil infiltration and tissue damage in septic lung damage. *Br. J. Pharmacol.* **172**, 5347–5359 (2015).
10. Lapchak, P.H. *et al.* The role of platelet factor 4 in local and remote tissue damage in a mouse model of mesenteric ischemia/reperfusion injury. *PLoS One* **7**, e39934 (2012).
11. Wetterholm, E., Linders, J., Merza, M., Regner, S. & Thorlacius, H. Platelet-derived CXCL4 regulates neutrophil infiltration and tissue damage in severe acute pancreatitis. *Transl. Res.* **176**, 105–118 (2016).
12. Zaldivar, M.M. *et al.* CXC chemokine ligand 4 (Cxcl4) is a platelet-derived mediator of experimental liver fibrosis. *Hepatology* **51**, 1345–1353 (2010).
13. Fricke, I., Mitchell, D., Petersen, F., Bohle, A., Bulfone-Paus, S. & Brandau, S. Platelet factor 4 in conjunction with IL-4 directs differentiation of human monocytes into specialized antigen-presenting cells. *FASEB J.* **18**, 1588–1590 (2004).
14. Scheuerer, B. *et al.* The CXC-chemokine platelet factor 4 promotes monocyte survival and induces monocyte differentiation into macrophages. *Blood* **95**, 1158–1166 (2000).
15. Marti, F. *et al.* Platelet factor 4 induces human natural killer cells to synthesize and release interleukin-8. *J. Leukoc. Biol.* **72**, 590–597 (2002).
16. Struyf, S. *et al.* Angiostatic and chemotactic activities of the CXC chemokine CXCL4L1 (platelet factor-4 variant) are mediated by CXCR3. *Blood* **117**, 480–488 (2011).
17. Liu, C.Y., Battaglia, M., Lee, S.H., Sun, Q.H., Aster, R.H. & Visentin, G.P. Platelet factor 4 differentially modulates CD4 + CD25 + (regulatory) versus CD4 + CD25- (nonregulatory) T cells. *J. Immunol.* **174**, 2680–2686 (2005).
18. Mueller, A. *et al.* CXCL4-induced migration of activated T lymphocytes is mediated by the chemokine receptor CXCR3. *J. Leukoc. Biol.* **83**, 875–882 (2008).
19. Vrij, A.A., Rijken, J., Van Wersch, J.W. & Stockbrugger, R.W. Platelet factor 4 and beta-thromboglobulin in inflammatory bowel disease and giant cell arteritis. *Eur. J. Clin. Invest.* **30**, 188–194 (2000).
20. Das, S., MacDonald, K., Chang, H.Y. & Mitzner, W. A simple method of mouse lung intubation. *J. Vis. Exp.* **73**, e50318 (2013).
21. Hashimoto, Y., Moki, T., Takizawa, T., Shiratsuchi, A. & Nakanishi, Y. Evidence for phagocytosis of influenza virus-infected, apoptotic cells by neutrophils and macrophages in mice. *J. Immunol.* **178**, 2448–2457 (2007).
22. Hufford, M.M. *et al.* Influenza-infected neutrophils within the infected lungs act as antigen presenting cells for anti-viral CD8(+) T cells. *PLoS One* **7**, e46581 (2012).
23. Tate, M.D., Brooks, A.G., Reading, P.C. & Mintern, J.D. Neutrophils sustain effective CD8(+) T-cell responses in the respiratory tract following influenza infection. *Immunol. Cell Biol.* **90**, 197–205 (2012).
24. Tate, M.D., Deng, Y.M., Jones, J.E., Anderson, G.P., Brooks, A.G. & Reading, P.C. Neutrophils ameliorate lung injury and the development of severe disease during influenza infection. *J. Immunol.* **183**, 7441–7450 (2009).
25. Tecle, T., White, M.R., Gantz, D., Crouch, E.C. & Hartshorn, K.L. Human neutrophil defensins increase neutrophil uptake of influenza A virus and bacteria and modify virus-induced respiratory burst responses. *J. Immunol.* **178**, 8046–8052 (2007).
26. Dienz, O. *et al.* Essential role of IL-6 in protection against H1N1 influenza virus by promoting neutrophil survival in the lung. *Mucosal Immunol.* **5**, 258–266 (2012).
27. Kobayashi, Y. Neutrophil infiltration and chemokines. *Crit. Rev. Immunol.* **26**, 307–316 (2006).
28. Wareing, M.D., Lyon, A.B., Lu, B., Gerard, C. & Sarawar, S.R. Chemokine expression during the development and resolution of a pulmonary leukocyte response to influenza A virus infection in mice. *J. Leukoc. Biol.* **76**, 886–895 (2004).
29. Wareing, M.D., Shea, A.L., Inglis, C.A., Dias, P.B. & Sarawar, S.R. CXCR2 is required for neutrophil recruitment to the lung during influenza virus infection, but is not essential for viral clearance. *Viral Immunol.* **20**, 369–378 (2007).
30. Konrad, F.M. & Reutershan, J. CXCR2 in acute lung injury. *Mediators Inflamm.* **2012**, 740987 (2012).
31. Garcia-Lopez, M.A. *et al.* CXCR3 chemokine receptor distribution in normal and inflamed tissues: expression on activated lymphocytes, endothelial cells, and dendritic cells. *Lab. Invest.* **81**, 409–418 (2001).
32. Raemdonck, K.V., Van den Steen, P.E., Liekens, S., Van Damme, J. & Struyf, S. CXCR3 ligands in disease and therapy. *Cytokine Growth Factor Rev.* **26**, 311–327 (2015).
33. Ichikawa, A. *et al.* CXCL10-CXCR3 enhances the development of neutrophil-mediated fulminant lung injury of viral and nonviral origin. *Am. J. Respir. Crit. Care Med.* **187**, 65–77 (2013).
34. Hartl, D. *et al.* Infiltrated neutrophils acquire novel chemokine receptor expression and chemokine responsiveness in chronic inflammatory lung diseases. *J. Immunol.* **181**, 8053–8067 (2008).
35. Eslin, D.E. *et al.* Transgenic mice studies demonstrate a role for platelet factor 4 in thrombosis: dissociation between anticoagulant and antithrombotic effect of heparin. *Blood* **104**, 3173–3180 (2004).
36. Srivastava, K. *et al.* Platelet factor 4 mediates inflammation in experimental cerebral malaria. *Cell Host Microbe* **4**, 179–187 (2008).